

# Low-Cost Sensing Platforms Based on Tunable 1D Photonic Crystals Integrated with Organic Light-Emitting Diodes and Photodetectors

I. Pavlichenko<sup>†,‡</sup>, A.T. Exner<sup>\*</sup>, P. Lugli<sup>\*</sup>, G. Scarpa<sup>\*</sup> and B.V. Lotsch<sup>†,‡</sup>

<sup>†</sup>Max Planck Institute for Solid State Research, Heisenbergstrasse 1, D-70569 Stuttgart, Germany

<sup>‡</sup>Department of Chemistry, Ludwig Maximilian University (LMU), Butenandtstrasse 5-13 (D), D-81377 Munich, Germany

<sup>\*</sup>Institute for Nanoelectronics, Technische Universität München, Arcisstrasse 21, D-80333 Munich, Germany

## ABSTRACT

Herein, we present an innovative detection platform based on utilizing one-dimensional photonic crystals (1D PCs) as responsive multilayers for intensity modulation of narrow-band light sources, namely, organic light-emitting diodes (OLEDs). The tunable range for the stop band modulation lies in the visible region and can thus be detected in a straightforward fashion by a visible-light photodetector or an image sensor (CCD). We propose a route towards the bottom-up assembly of a fully functional, integrated miniature platform with a resolution exceeding the capabilities of most commercial spectrometers, and show temperature, humidity and chemical analyte detection.

**Keywords:** sensors, one-dimensional photonic crystals, OLED, photodiode

## 1 INTRODUCTION

Photonic crystal (PC) research has been flourishing over the past years, giving a rise to a development of photonic crystal building blocks for a variety of optical systems, for example, in optical fibers, switches and waveguides, lasers, color displays and others.<sup>1,2</sup> Among the various types of PC structures *stimuli-responsive* photonic crystals have garnered special attention as they further

boost the range of applications toward tunable optical filters, which are able to dynamically respond to external environmental stimuli through optical thickness changes.<sup>3</sup> A promising area of applications of stimuli-responsive PCs is the development of label-free biological, chemical, and physical colorimetric sensors.<sup>4</sup> The sensing approach is based on the implementation of PCs as tunable optical filters capable of changing their refractive properties when in contact with an analyte of interest or when exposed to external stimuli such as electric and magnetic fields, pH, etc.

Among the various types of PCs a particular focus is on conceptually simple and versatile one-dimensional PCs.<sup>5</sup> 1D PCs are interference-based multilayered nanostructures consisting of a periodic assemblage of layers of two different materials featuring high and low refractive indices ( $n$ ), respectively. The periodicity of the dielectric permittivity of the multilayer structure affects photons in the same way as the periodic potential in a semiconductor crystal affects the electron motion, leading to the phenomenon that photons with particular energies cannot propagate within the PC. A resulting wavelength range, in which the incident photons are being reflected from the PC, is called a photonic band gap or stop band. The central wavelength ( $\lambda_{Bragg}$ ) of the stop band can be calculated by the Bragg-Snell law for normal incidence (Equation 1):

$$m\lambda_{Bragg} = 2(n_H d_H + n_L d_L) \quad (1)$$

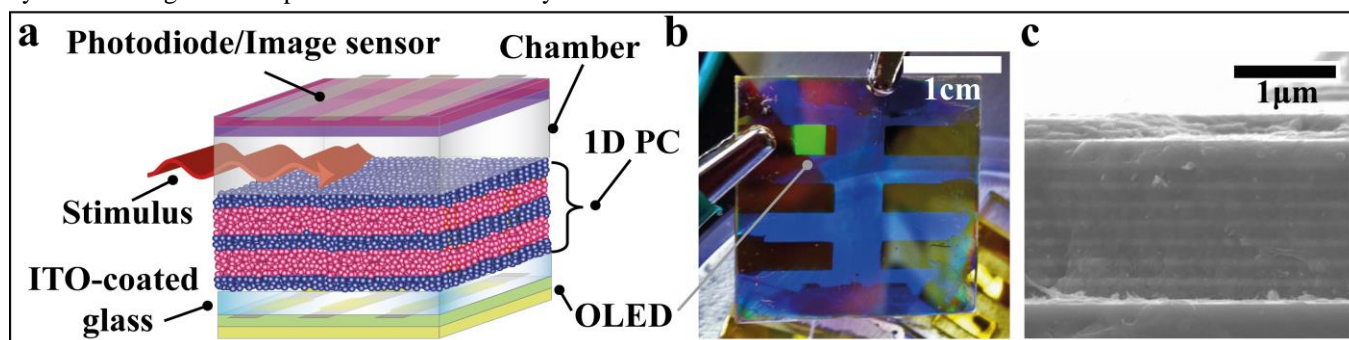


Figure 1: a) Scheme of the proposed detection platform: An OLED fabricated on the ITO-coated side of the glass substrate emits through the responsive 1D PC, which is exposed to a certain stimulus or analyte. The modulated intensity of light is detected by an photodetector or an image sensor. b) Photograph of the OLED - 1D PC ensemble, shown in Figure 1a. The OLED area can be seen as a green square on the upper left corner. c) Cross-section SEM image of the 1D PC, composed of 9 nanoparticle-based SiO<sub>2</sub> (dark layers)/TiO<sub>2</sub> (bright layers) bilayers.

where  $m$  is the diffraction order and  $n_H$ ,  $n_L$ ,  $d_H$ , and  $d_L$  are the respective refractive indices and thicknesses of the high- (H) and low- (L) refractive index (RI) materials. As can be seen from Equation 1, the position of the stop band can be modulated by varying the optical thickness (the product of RI and physical thickness) of the layers.<sup>6,7</sup> The sol-gel chemistry provides simple, fast, and low-cost synthetic pathways to produce nanoparticles for the assembly of 1D PCs with high optical and structural quality by spin-coating.<sup>8</sup>

A color change of the PC is typically detected by a spectrometer or by the naked eye, which, however, may give rise to uncertainties. Rationally, such sensor must be able to transform the optical change into an electrical signal. Therefore, signal transduction mechanisms allowing to convert the environmental response of a tunable PC into an electronic signal are of great interest.<sup>9</sup> Besides, other important factors for sensor production are low cost, low energy consumption and small dimensions, a non-complex read-out, and high sensitivity with a high signal-to-noise ratio.<sup>10</sup>

Following this incentive, we report a *modus operandi* towards producing a sensor platform with a ternary architecture based on the integration of solution-processed stimuli-responsive one-dimensional photonic crystals with a narrow-band light source, namely, an organic or inorganic light-emitting diode (OLED and LED, respectively), and with a photodiode or a high-resolution camera.<sup>9,10</sup> The sensing principle is based on visualizing the changes of the intensity of light, propagating from the light source through the 1D PC. Detecting visible light can be done in a straightforward and inexpensive fashion with low noise by using a solution processed organic photodiode or commercially available CCD or CMOS imagers. In this respect, our approach surpasses the standard photonic crystal detection schemes based on the registration of the spectral shift of the photonic stop band. The proposed setup is compatible with every PC exhibiting a change of stop-band position and/or transmission in the visible range, demonstrating the versatility of the proposed concept.

## 2 RESULTS AND DISCUSSION

The scheme of the proposed sensing platform shown in Figure 1a features a stimuli-responsive optical element – the 1D photonic crystal – incorporated between a photodiode and a narrow-band light source, e. g. an OLED. This “sandwich” architecture acts like a transducer, translating the optical response of the 1D PC into an electrical signal. Figures 1b depict a photographic image of the 1D PC deposited onto the ITO glass substrate and integrated with a polymer OLED, assembled by spin-coating. The fabrication of the OLED and PC on the same substrate greatly reduces the system complexity. The 1D PC usually consists of 6 to 9 bilayers of mesoporous nanoparticle-based TiO<sub>2</sub> and SiO<sub>2</sub> featuring a pronounced photonic stop-band due to the high RI contrast of the layers.

Figure 1c outlines a SEM micrograph of the layer morphology, showing the TiO<sub>2</sub> as bright stripes and the SiO<sub>2</sub> as dark stripes. The choice of the layer thicknesses of the 1D PC is dictated by the emissive properties of the used OLED (based on the polymer PDY-132), which has an

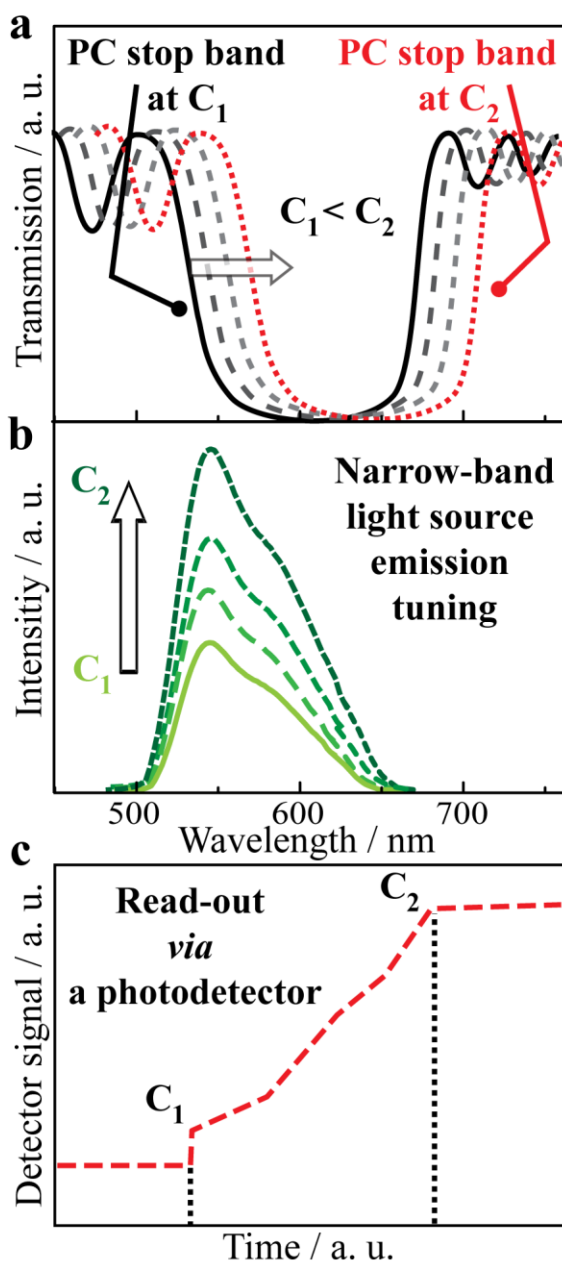


Figure 2: Schematic illustration of the detection principle. a) The transmission spectra of the 1D PC corresponding to various gas concentrations between  $C_1$  and  $C_2$  ( $C_1 < C_2$ ), b) The emission spectra of the OLED shining through the 1D PC (as shown in Figure 1b). A PC exposed to an analyte concentration  $C_1$  transmits less incident OLED light compared to the PC at a higher concentration  $C_2$ . c) The corresponding change of OPD current, resulting from the increase in the intensity of the transmitted light.

emission intensity maximum of 550 nm, and results from an

optimization procedure towards a maximised response of transmitted light for a given stop-band shift.

The influence of the position of the photonic stop-band on the light intensity is schematically demonstrated in Figure 2 using the example of chemical sensing. Figure 2a shows the photonic stop-band positions corresponding to different vapor concentrations ( $C_1 < C < C_2$ ) and Figure 2b the emission spectra of the OLED measured for the corresponding concentrations. The stop-band shift – a measure of the analyte concentration - is then derived by comparing the initial photodiode signal without analyte exposure to the value that is measured during exposure, as shown in Figure 2c.

## 2.1 Chemical sensing

As a proof of concept, we demonstrate the universality of the proposed approach by using a commercially available narrow-band green LED as light emitter and the Si-based slim photodiode power sensor from Thorlabs. By detecting the light intensity transmitted through the 1D PC as a function of analyte concentration, the chemo-tunability of the PC directly translates into the intensity modulation observed at the detector.

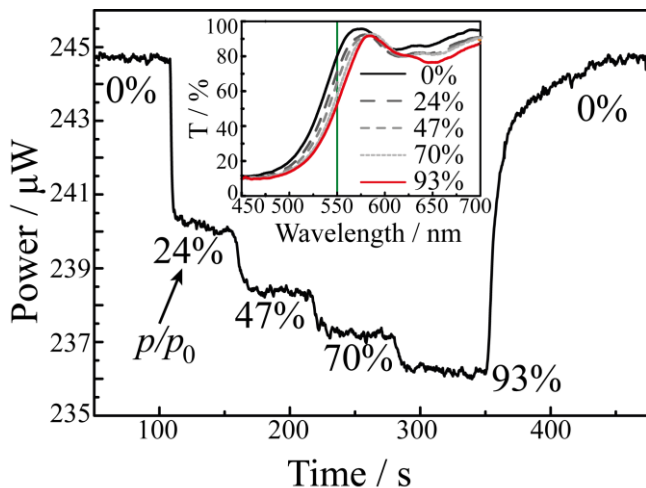


Figure 3: Response curve of the proposed sensor to changes in the relative pressure of the water vapor vapor from 0 to 93%. The inset graph: Transmission spectra of the 6 bilayer  $\text{TiO}_2$  (60 nm)/ $\text{SiO}_2$  (90 nm) 1D PC taken under normal incidence of light, demonstrate a red shift ( $\approx 18$  nm) for relative water pressures ( $p/p_0$ ) from 0 to 93%.

Figure 3 demonstrates a time-resolved response curve of the powermeter to the changes in the relative pressure ( $p/p_0$ ) of the water vapor supplied into a miniature polydimethylsiloxane chamber (schematically shown in Figure 1a) which isolates the system from ambient air and guides the analyte vapor mixture over the surface of the BS through an in- and outlet hole. Notably, the optical power of the LED has diminished upon the increase of  $p/p_0$  from 0 to 93% from 245  $\mu\text{W}$  down to 236  $\mu\text{W}$ . This can be

explained by the tuning behaviour of the mesoporous 1D PC induced by the analyte infiltration. As can be seen in the inset of the Figure 3, the red side of the photonic stop band shifts to longer wavelengths by  $\approx 18$  nm, inducing the decrease in the set of the transmission values corresponding to the maximum wavelength of the LED of 550 nm. The presented setup is generic and can detect optical changes in the transmission of PCs, which can be induced by both vapor adsorption or by a liquid analyte as demonstrated with a microfluidic setup.

## 2.2 Temperature sensing

In order to demonstrate the possibility of IR imaging we integrated the OLED-1D PC sensor with an image sensor, as indicated in the scheme in Figure 4 a.<sup>10</sup> We set up a commercial CCD camera above the device so that the light output can be measured over the whole OLED-1D PC area with a resolution of 530 by 530 pixels. To detect the filter transmission in two dimensions, the light emission had to be homogeneous over the whole active filter area, a criterion provided by the chosen OLED geometry. To perform the intensity modulation of the light emitted by the OLED, we assembled a 1D PC consisting of 6 bilayers of nanoparticle-based  $\text{TiO}_2$  and  $\text{SiO}_2$  layers. The optimization of the thickness of the layers (60 nm for  $\text{TiO}_2$  with  $\text{RI} \approx 1.9$  and 110 nm for  $\text{SiO}_2$  with  $\text{RI} \approx 1.3$ ) allowed us to obtain a filter with a first order photonic stop band between 490 and 640 nm, matching the emission spectrum of the polymer OLED lying in the range between 500 and 620 nm. Heating induces a change in the effective RI of the employed materials due to the combination of two phenomena operating simultaneously: The inherent thermo-optic effect and the desorption of the water molecules from the porous network of the BS, leading to a change of the optical thickness of the layers, and, thus, to a blue shift of the stop band position. We observed a blue shift of the stop band position equal to 25 nm upon increasing the temperature, from 15  $^\circ\text{C}$  to 35  $^\circ\text{C}$ .

In Figure 4b we present a colored optical image of the OLED-BS equilibrated at 27  $^\circ\text{C}$ . The light intensity is relatively constant over the whole 3 x 3 mm large surface. The actual gray-scale image as acquired from the CCD camera is shown in the upper right corner. Figure 6 c shows a colored optical image of the OLED-BS under a temperature gradient induced by a hot source generating a local temperature of less than 60  $^\circ\text{C}$  on the edge of the device. Figure 6 d is taken 10 seconds after heating, when the device was at a temperature of 33  $^\circ\text{C}$ . Thus, we prove that with the proposed thermo-optic intensity-tuning technique one can visualize the temperature changes of the integrated optical systems with an image sensor such as a CCD array. Furthermore, one can time and spatially resolve the kinetics of thermal equilibration and spreading of temperature fronts in the OLED-BS coupled devices.

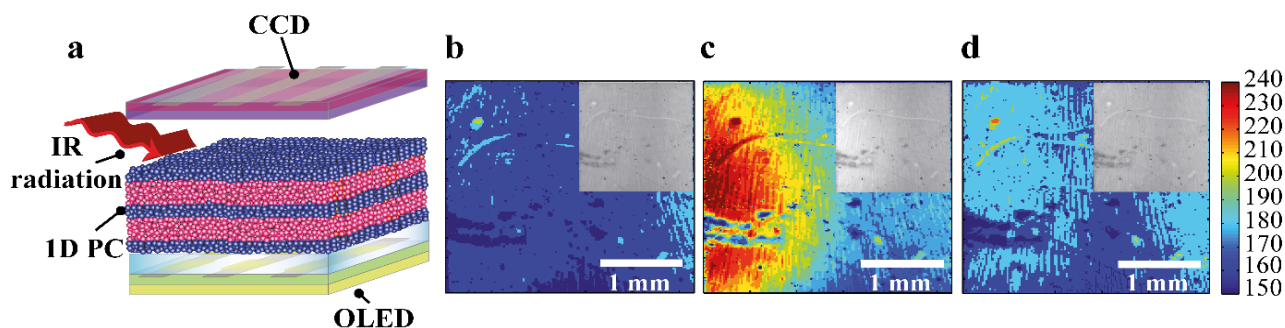


Figure 4: a) Scheme of the setup used for the IR imaging. Colored optical images demonstrating the OLED shining through the BS in b) thermal equilibrium at 27 °C and c) heated on the left side, c) 10 seconds after heating at a temperature of 33 °C. b-d reproduced with permission.<sup>9</sup> The insets show the corresponding raw image obtained by a monochrome CCD camera.

### 3 CONCLUSION

In conclusion, we demonstrate a generic low-cost sensing platform based on tunable 1D PCs integrated with organic and inorganic light-emitting diodes and photodetectors, which is able to convert the color shift of a stimuli-responsive 1D PC into an electric signal. Furthermore, we show that the local stimulus distribution profile can be time and spatially resolved, thus enabling potential applications as imaging sensors featuring low power consumption, straightforward assembly methods and low fabrication costs.

[10] A. T. Exner, I. Pavlichenko, B. V. Lotsch, G. Scarpa and P. Lugli, *ACS Appl. Mater. Interfaces*, 5, 1575–1582, 2013.

### REFERENCES

- [1] Inoue and Ohtaka " Photonic Crystals: Physics, Fabrication and Applications," Springer, 2004.
- [2] A. C. Arsenault, D. P. Puzzo, I. Manners and G. A. Ozin, *Nat. Photonics* 1, 468 – 472, 2007.
- [3] Yin "Responsive Photonic Nanostructures: Smart Nanoscale Optical Materials," The Royal Society of Chemistry, 2013.
- [4] C. Fenzl, T. Hirsch and O.S. Wolfbeis, *Angew. Chem. Int. Ed.*, 53, 3318 – 3335, 2014.
- [5] Joannopoulos, Johnson, Winn and Meade "Photonic crystals: Molding the flow of light," Princeton University, 2nd ed., 44-65, 2008.
- [6] L. D. Bonifacio, B. V. Lotsch, D. P. Puzzo, F. Scotognella and G. A. Ozin, *Adv. Mater.*, 21, 1641–1646, 2009.
- [7] M. E. Calvo, S. Colodrero, N. Hidalgo, G. Lozano, C. López-López, O. Sánchez-Sobrado and H. Míguez, *Energy Environ. Sci.*, 4, 4800, 2011.
- [8] G. von Freymann, V. Kitaev, B. Lotsch and G. A. Ozin, *Chem. Soc. Rev.*, 42, 2528–2554, 2013.
- [9] A. T. Exner, I. Pavlichenko, D. Baierl, M. Schmidt, G. Derondeau, B. V. Lotsch, P. Lugli and G. Scarpa, *Laser Photon. Rev.*, 2014.